International Journal of Fluid Power 8 (2007) No. 3 pp. 31-41

OPTIMISATION OF FLOW THROUGH A PNEUMATIC CONTROL VALVE USING CFD ANALYSIS AND EXPERIMENTAL VALIDATION

Nicholas Paul Whitehead[1], Arezki Slaouti[2] and Howard Taylor[2]

[1] *Bifold Fluidpower Ltd., Greenside Way, Middleton, Manchester, M24 1SW, UK*
[2] *Department of Engineering and Technology, Manchester Metropolitan University, John Dalton Building, Chester Street, Manchester, M1 5GD, UK*
nwhitehead@bifold-fluidpower.co.uk, a.slaouti@mmu.ac.uk, h.taylor@mmu.ac.uk

Abstract

Computational Fluid Dynamics (CFD) is becoming a tool that can be used by engineers to optimise valve performance. CFD is used here to model the fluid flow characteristics through a control valve. By changing various aspects of the internal flow path, the performance of a valve is improved through a greater mass flow rate to optimise its performance. These changes included rounding sharp edges, removing areas of dead-space and moving some internal parts to reduce sharp changes in direction. The CFD model was used to create a new modified design which was then manufactured for testing. The test results were compared to the CFD results from the new model. The CFD and experimental results showed a similar increase in flow rate from the original to the modified valve showing that changes to the internal flow path had a positive effect on the measured flow rate.

Keywords: computational fluid dynamics; pneumatic control valve

1 Introduction

For this paper a solenoid operated pneumatic control valve, manufactured by Bifold Fluidpower, was considered. It shall be referred to as valve X throughout this paper. Figure 1 shows a photograph of valve X with a manual reset solenoid and Fig. 2 shows a section view of valve X with the solenoid operator removed. The valve contains a central spool assembly with captivated o-rings for sealing on the valve seats. When the solenoid is passive, the spool assembly is held in the closed position by the spring. In the closed position the upper o-ring seals on the upper seat face and fluid can pass between ports 2 and 3. When operated, the solenoid pushes the spool down onto the opposite seat and allows fluid to pass between ports 1 and 2. Figure 3 shows the flow path in its two positions. Valve X has a range of strokes depending on the solenoid fitted. They range from 0.6 to 1.2 mm. A valve with 0.6 mm stroke was considered for this project.

This manuscript was received on 21 March 2007 and was accepted after revision for publication on 10 October 2007

Fig. 1: *Photograph of valve X, showing the valve body and a manual over ride solenoid*

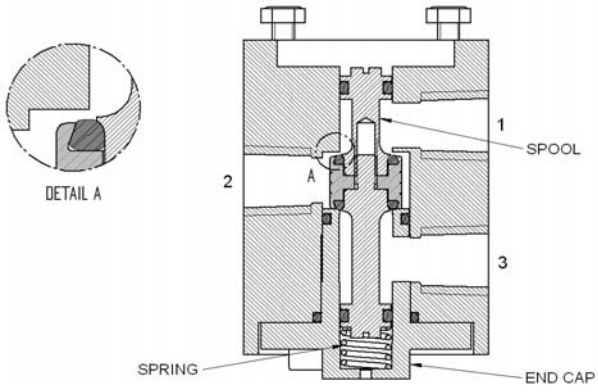

Fig. 2: *Section view through valve X, shown when the solenoid is operated*

© 2007 TuTech

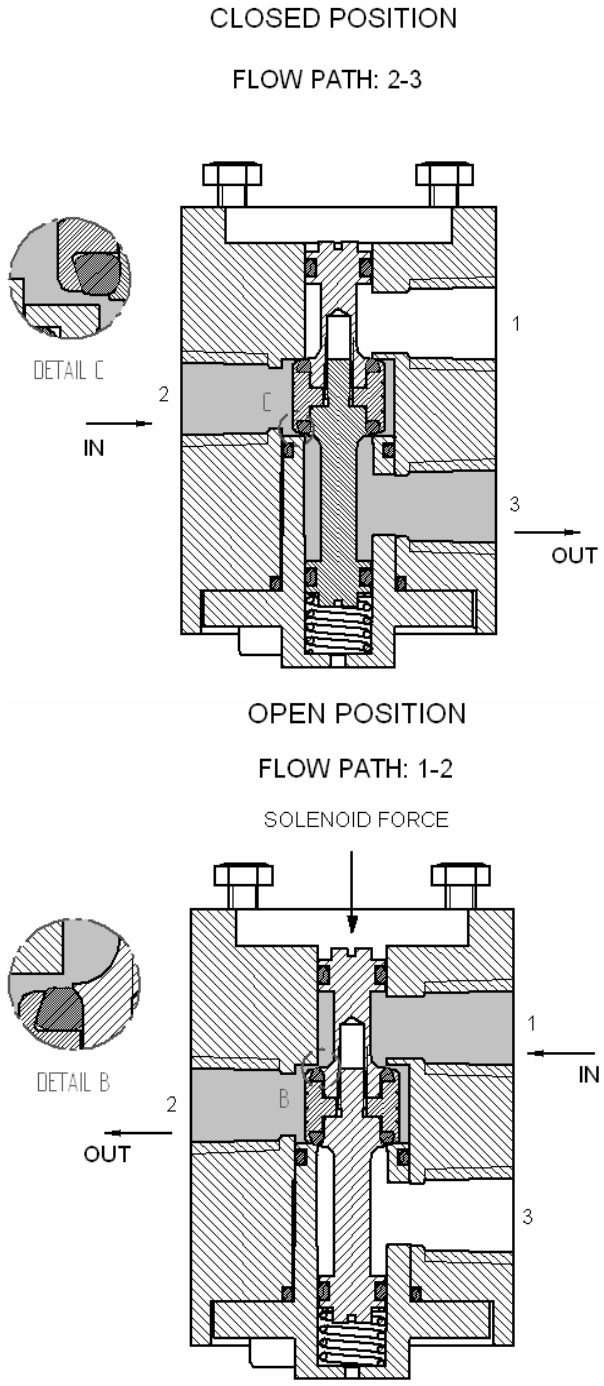

Fig. 3: *Section view through valve X, showing the flow path in its two positions*

Valves of this type are typically designed and developed using past experience and trial and error through design, manufacture and testing. Test results are recorded manually and little theory or advanced design techniques are implemented during the design process. Traditionally, assessment of the effect of valve design on flow performance has been conducted rather empirically (Sullivan 1975; Yeaple 1990). Empirically-based equations were developed by valve manufacturers through experimentation and trial and error. The performance of hydraulic control valves is now well documented and better understood but no real theoretical models are available due to the very complex fluid-body parts interaction within the valve. In the case of pneumatic control valves, compressibility of the gas makes it an even harder task. Previous work (Sullivan 1975; Yeaple 1990) has also predominantly been directed towards valves with larger bore diameters and orifices, so relatively little is known on the performance of smaller pneumatic control valves, such as the one considered in this paper.

Over the past few years, the use of CFD in the design and simulation of control valves has increased considerably. Initially, valves were simplified and modelled as two-dimensional (Kerh et al., 1997) or axisymmetrical (Davis and Stewart 2002). Three-dimensional valves also had their geometries simplified for their corresponding CFD simulation (Min et al., 2001; Bredau and Helduser 1999). Using CFD, various types of valves were thus simulated: poppet valves (Ito et al., 1993; Nadarajah et al., 1998), spool valves (Min et al., 2001) and butterfly valves (Huang and Kim 1996). These simulations reproduced the main characteristics of the flow through the simplified valves. However, no real valve with its full internal geometry was simulated. Salvador and Valverde (2004) carried out a CFD simulation of a control valve with a complex geometry but struggled with its full simulation and ended up splitting the simulation into three successive parts. This paper considers the CFD simulation of the control valve with its full three-dimensional complexity. This has recently been made possible with the ease of importing the full corresponding CAD geometry of a complex object into a CFD package. Also, as the CFD packages (such as CFX and Fluent) have become quite accurate in their results (conservation of mass flow rate and accurate reproduction of boundary layers and separated flow regions) such a simulation will indicate the intricate features of the flow within the complex internal passages of the valve. Alterations will then be made to selected parts of the internal geometry of the valve in order to improve the performance of the valve by increasing the mass flow rate of the fluid through it (for a given pressure difference) which is the main improvement required here. As the main parts involved in the workings of the valve (seat, seals, stroke etc...) are not altered, the redesigned valve will benefit from a smoother fluid flow and less pressure loss through its internal passages. The improved valve is then to be manufactured and tested experimentally for its improved performance. Such a procedure (CFD simulation, improvement of model through CFD trials, redesign and manufacturing of improved model and finally, confirmation of improvement in new model through experimental testing) is likely to be the trend when using complex parts that deal with fluid flow.

2 CFD Simulations

2.1 CFD Modelling

A number of cases were modelled using ANSYS CFX. For each model an inlet and outlet pressure of 6 and 5 bar(g), respectively, were applied. This standard pressure difference of 1 bar is used for both the CFD simulation and the corresponding experimental testing. Our results showed that the flow through the valve un-

der these conditions remain subsonic. Although real conditions of use for these valves are expected to be different they will not vary much from these conditions as the outlet of the valve will not be at a much lower pressure than that of the inlet. Under operational use the pressure difference across the valves will be more controlled by the amount of pressure loss through the valve than by the back pressure of the system which will be a long way further downstream of the valve outlet. As such, the corresponding flow rate through the valve can be used as a good indicator for the performance of the valve. The shear stress transport model (SST) was used to model turbulence. This particular model, designed to give a high accurate prediction of the onset and the amount of flow separation under adverse pressure gradients, is quite appropriate for complex internal flows (Bardina et al., 1983). Air was used as the fluid domain and compressibility effects were implemented using the Ideal Gas Law. The full Navier-Stokes equations (continuity equation, three-dimensional momentum equation and energy equation) were solved in conjunction with the turbulence model to yield computed results for the three velocities, pressure, density, Mach number and turbulence quantities. The CFX solver uses a high resolution advection scheme. The convergence criterion was set at 10^{-4} and the maximum number of iterations was set at 1000. A typical computing time for the converged flow through the valve was about 4 hours.

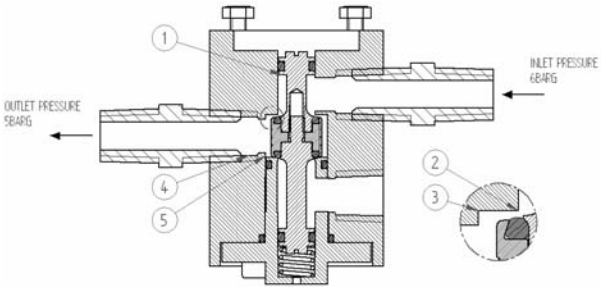

Fig. 4: *Cross section through the imported geometry of flow through ports 2-3*

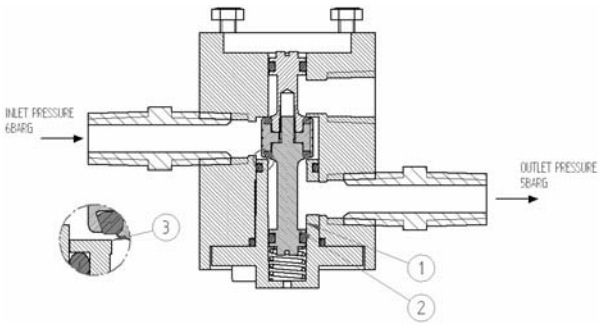

Fig. 5: *Cross section through the imported geometry of flow through ports 1-2*

Figures 4 and 5 show cross sections through the imported geometry for flow through the valve in its closed and open positions respectively (ports 2-3 and 1-2). In each case, the solid model was imported into ANSYS CFX and the flow domain subtracted from the model. The valve fittings shown in Fig. 4 and 5 were included in the model to obtain the closest representation to experimental testing as possible. An unstructured tetrahedral mesh was used in the analysis. Figure 6 shows the face mesh of the valve and Fig. 7 shows the detailed view of the mesh inside the valve near the seat where a denser mesh was used because of the highly varying flow near to the valve seat. A total number of just over 300,000 elements was sufficient to produce an accurate simulation of the internal flow.

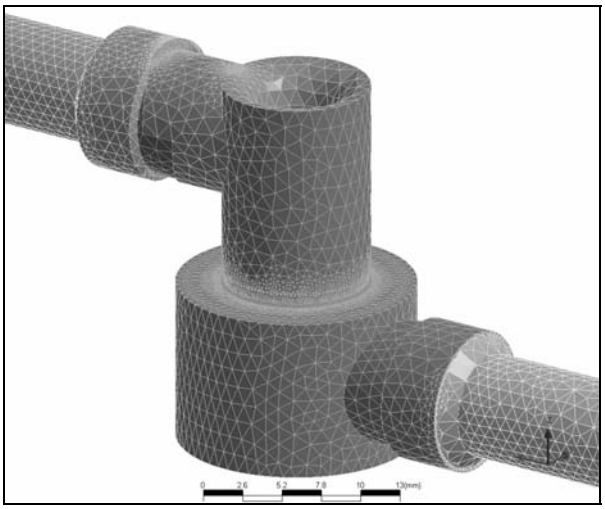

Fig. 6: *Face mesh of the valve*

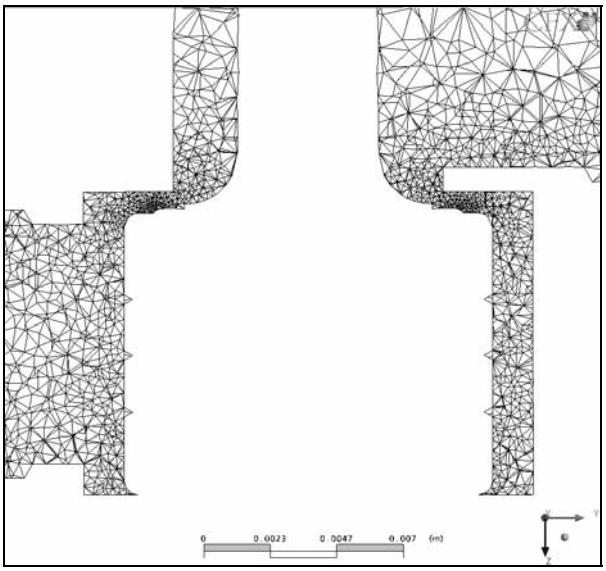

Fig. 7: *Mesh in central plane of the valve*

2.2 Changes to Internal Flow Path

Changes were gradually made to the internal flow path of the valve and the maximum flow rate was measured after each change. This was done using the CFD post processor. The following changes were made throughout the process:

2.2.1 Flow Through Valve, Ports 1-2

Case 1: Original design

Case 2: Top dead-space removed

In this case, the dead-space was removed from the top end of the stem (item 1 in Fig. 4).

Case 3: Top and bottom dead-space removed

In this case, the dead-space was removed from the

top end of the stem and the seat (item 1 and 5 in Fig. 4).

Case 4: Rounded edges

In this case, the edges around the poppet seat were rounded around the poppet seat (item 2 and 3 in Fig. 4).

Case 5: Top and bottom dead-space removed and rounded edges

In this case, the alterations from case 3 and 4 were combined.

Case 6: Top and bottom dead-space removed, rounded edges and port moved up

In this case, the alterations from case 5 were used and port 2 was moved up to fall in line with the seat face (item 4 in Fig. 4)

2.2.2 Flow Through Valve, Ports 2-3

Case 7: Original design

Case 8: Dead-space removed

In this case, the dead-space was removed from the top end of the stem (item 1 in Fig. 5).

Case 9: Rounded edges

In this case, the edges around the poppet seat were rounded around the poppet seat (item 3 in Fig. 5).

Case 10: Dead-space removed and rounded edges

In this case, the alterations from case 8 and 9 were combined.

Case 11: Dead-space removed, rounded edges and rounded spool

In this case, the alterations from case 10 were used and the bottom end of the stem was rounded (item 2 in Fig. 5)

2.3 CFD Results

Figures 8 and 9 show cross sections through the geometry for each case from ports 1-2 and 2-3 respectively. The velocity vectors are shown for each case on a central Y-Z plane through the valve along the direction of flow. Table 1 shows the corresponding mass flow rates in kg/s for each case.

For both sets of figures, the general flow characteristics are as would be expected with the flow from the inlet redirecting itself through the shape of the internal chamber towards the outlet. The shape of the internal chamber is critical, especially within the narrow annular passage where the velocities are the highest. The general rule for the velocity magnitude being inversely proportional to its corresponding cross-sectional area is observed in most cases, apart from those areas where flow separation occurs with flow recirculation taking place.

Figure 8a shows the internal flow through the original valve. Figures 10 and 11 show the corresponding contours of density and Mach number, respectively, for the same case. The compressibility effects are evident. It can be checked that the flow remains subsonic even through the narrow passages. Using the mass flow rate through the valve, one can calculate that the flow through the seat orifice has velocities close to the average of about 100 m/s. The correspondence between the velocity vectors and the Mach number contours and that between the density contours and the pressure contours are evident. All simulations obtained for the other cases were similarly realistic.

Case 1 shows the geometry of the original valve. Recirculation can be seen around the bottom seat; at the top of the outlet port near the outlet and at the top of the valve around the spool. In case 2, the dead space at the top of the valve has been removed and the recirculation is reduced in this area. In case 3, both the dead space at the top and bottom of the geometry has been removed and the recirculation has been reduced in these areas. In case 4, the edges have been rounded around the seat orifice. This has caused the flow to separate from the edge of the spool near the seat orifice and move towards the outlet sooner than in case 1. In case 5, all previous changes have been incorporated and similar effects can be seen as in the previous cases. In case 6, all previous changes have been incorporated and the outlet port has been moved upwards, in line with the top seat face. Similar effects can again be seen. Also recirculation has been reduced at the top of the outlet port near the outlet.

Case 7 shows the geometry of the original valve. Flow exits the seat orifice and is directed downwards. At the bottom of the valve, there is recirculation and flow is directed back towards the seat on the opposite side of the spool. In case 8, the dead space has been removed and the recirculation and upwards flow has been reduced. In case 9, the edges have been rounded around the seat orifice. Relatively little can be seen from the velocity vectors, but the mass flow has increased from case 8 to 9. In case 10, the previous changes have been incorporated and similar effects can be seen as in the previous cases. In case 11, all previous changes have been incorporated and the spool has been rounded at the bottom of the valve. Similar effects can again be seen. Also flow hits the rounded edge and is directed towards the outlet.

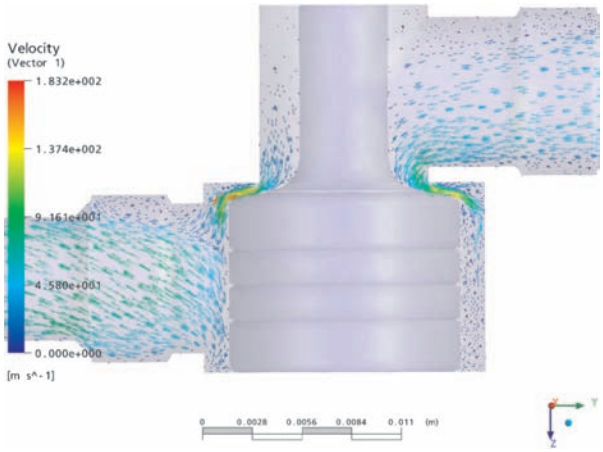

Fig. 8a: *Case 1*

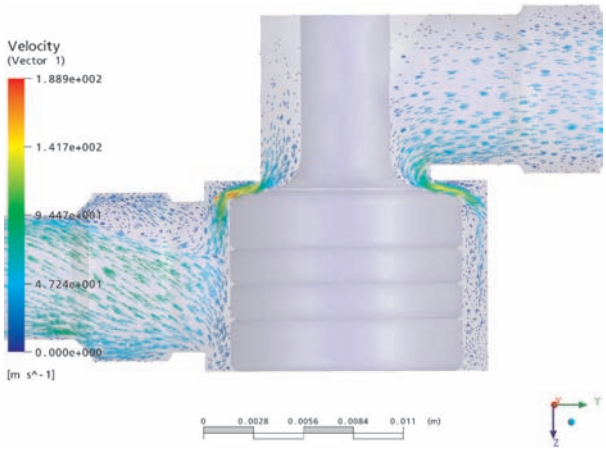

Fig. 8b: *Case 2*

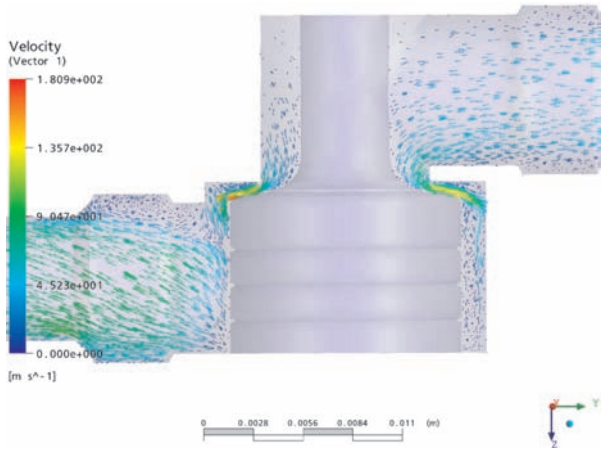

Fig. 8c: *Case 3*

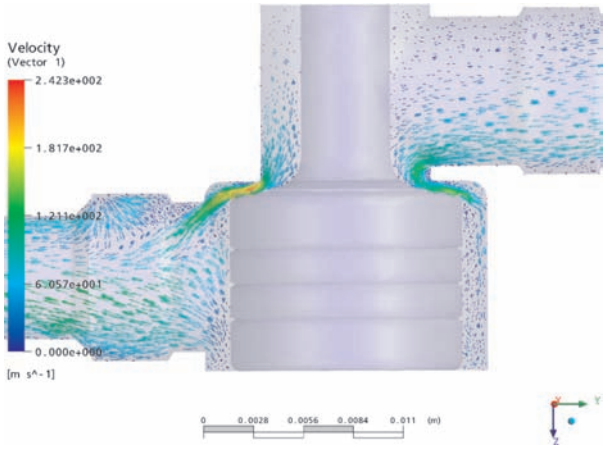

Fig. 8d: *Case 4*

Fig. 8a-8d: *CFD results: flow through valve, ports 1-2*

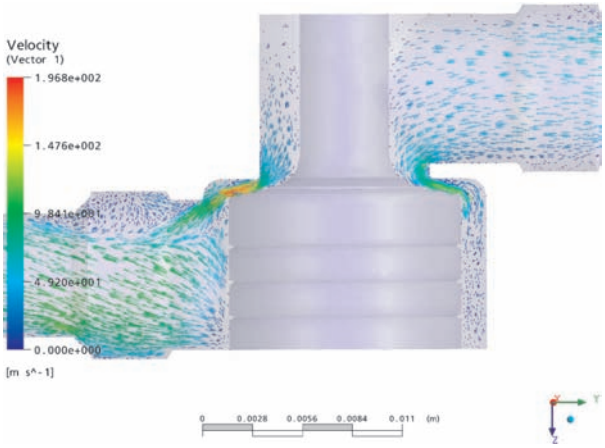

Fig. 8e: *Case 5*

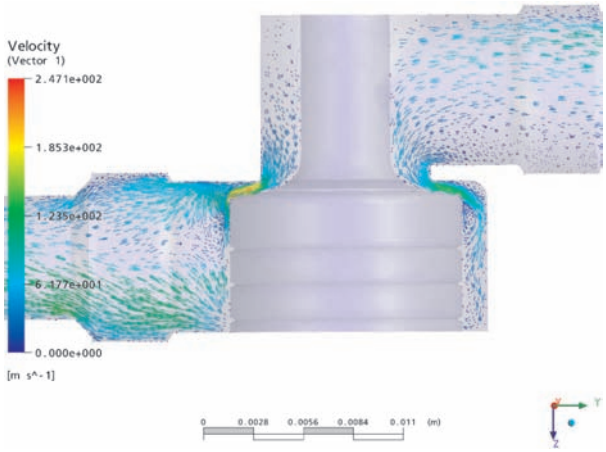

Fig. 8f: *Case 6*

Fig. 8e-8f: *CFD results: Flow through valve, ports 2-3*

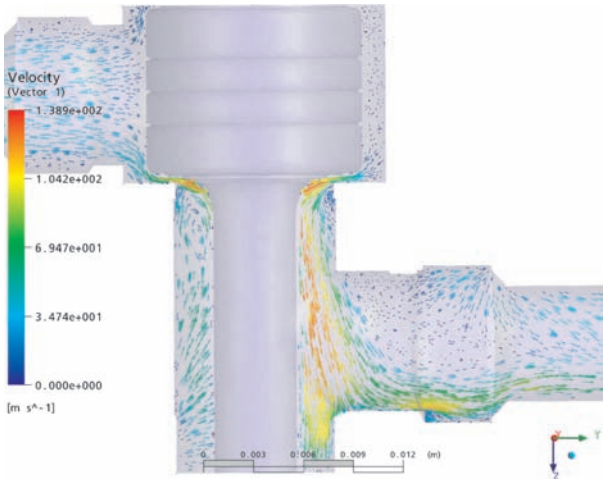

Fig. 9a: *Case 7*

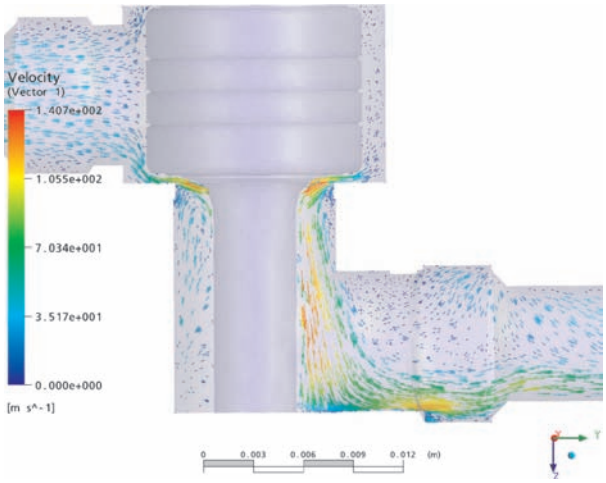

Fig. 9b: *Case 8*

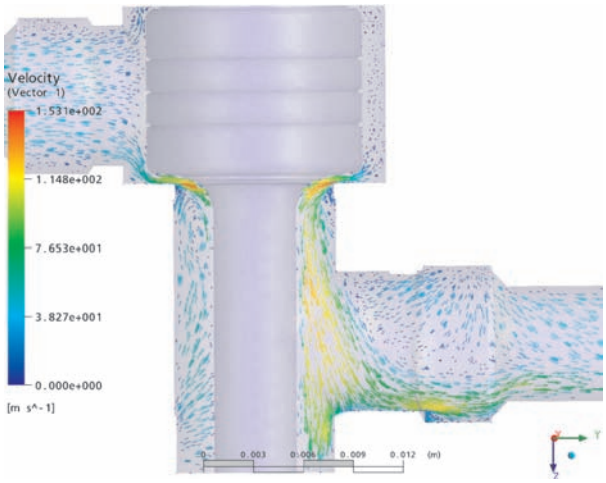

Fig. 9c: *Case 9*

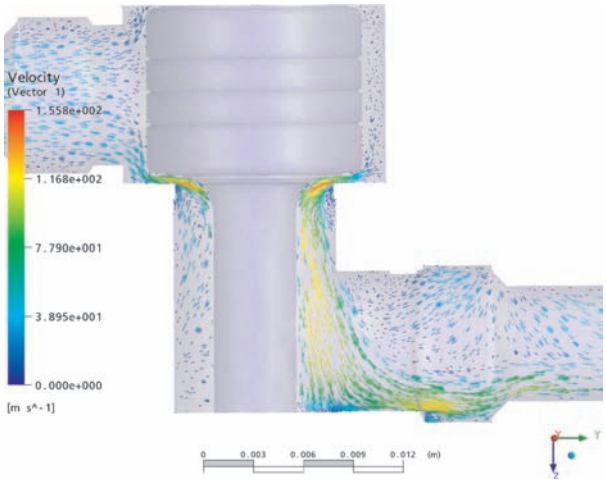

Fig. 9d: *Case 10*

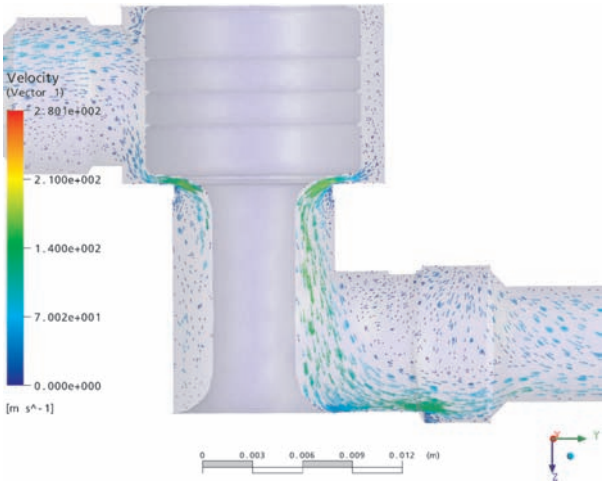

Fig. 9e: *Case 11*

Fig. 9: *CFD results: flow through valve, ports 2-3*

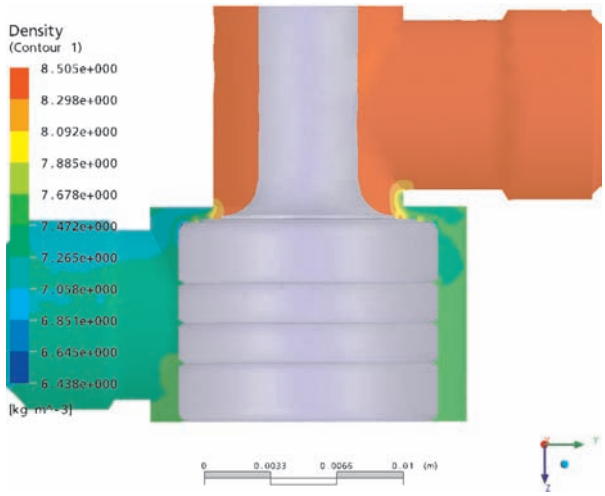

Fig. 10: *Density contours for case 1*

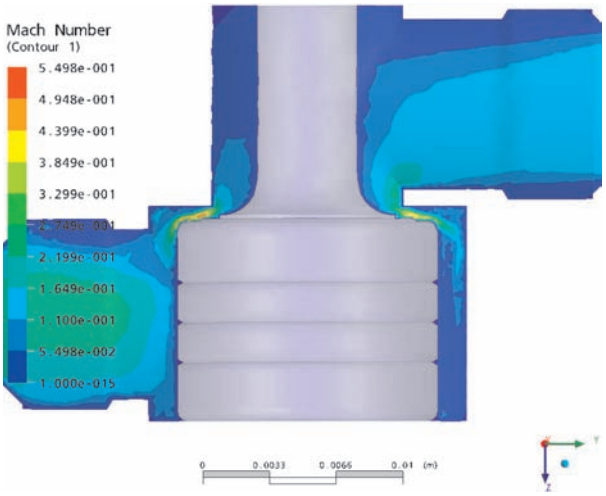

Fig. 11: *Mach number contours for case 1*

Table 1: Numerical results

Case	Mass flow (kg/s)	% Improvement
1	0.01600	0
2	0.01609	0.57
3	0.01589	-0.71
4	0.02153	34.55
5	0.01892	18.26
6	0.01897	18.54
7	0.01277	0
8	0.01284	0.59
9	0.01386	8.55
10	0.01396	9.34
11	0.01417	10.95

2.3 Final Design

A modified CAD model of valve X was created, incorporating the changes to the internal flow path that yielded the highest percentage improvement. Altering aspects of the flow to the extent shown in some of the previous cases would impact on the valves function, so for the final design, attention was paid to the function of the valve and the ability to machine its components. Using aspects of certain cases meant that others could not be used. For example, Item 2 in Fig. 4 was used, but item 3 was not as the port was moved level with the seat as in case 6. Figure 12 shows a cross section through the modified valve.

A working valve was manufactured from the model for experimental testing and the final geometry was imported into CFX for fluid flow modelling. Pneumatic and hydraulic results were obtained using air (ideal gas) and water respectively. Figure 13 shows the pneumatic CFD results from modelling the modified valve. Simu-lations of the original geometry (cases 1 and 7) were also run using water to compare the pneumatic and hydraulic results.

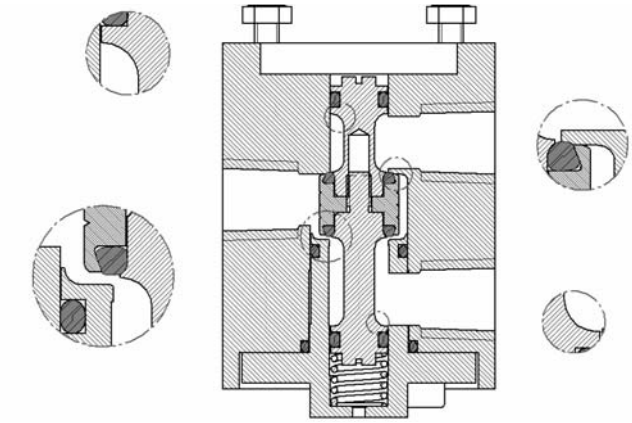

Fig. 12: *Cross section through the modified valve*

2.4 CFD Results from final design

Figures 13a and 13b show the cross sections through the geometry for the modified valve from ports 1-2 and 2-3 respectively. The velocity vectors are again shown for comparison. Table 2 shows the mass flow rate in kg/s for the existing design (valve A) and the modified design (valve B) in each direction.

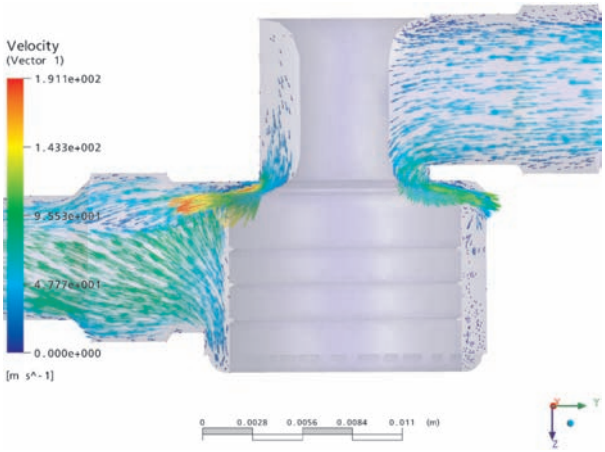

Fig. 13a: *CFD results of valve B ports 1-2*

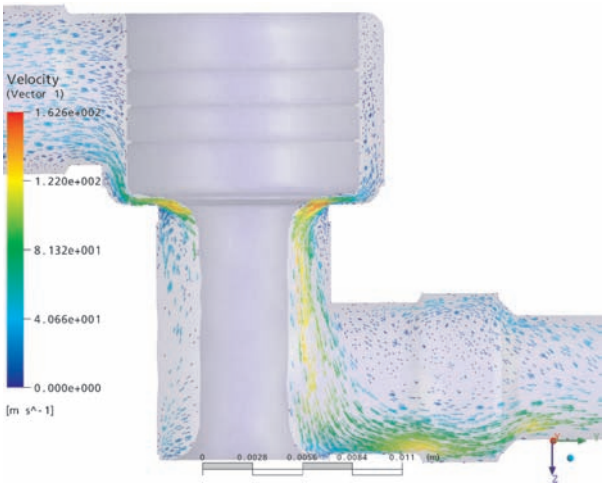

Fig. 13b: *CFD results of valve B ports 2-3*

Table 2: Comparison of CFD results

Ports	Flow (kg/s)		% difference
	Valve A	Valve B	
1-2	0.01600	0.01805	12.8
2-3	0.01277	0.01502	17.6

3 Experimental Testing

The existing valve (valve A) and modified valve (valve B) were tested on the following experimental test rigs:

- Pneumatic flow test
- Pneumatic actuator test
- Hydraulic flow test

3.1 Pneumatic Flow Test

Figure 15 shows the pneumatic flow test bench with valve X located in the centre of the photograph between the two electronic pressure transmitters. A flow rig that conformed to ISO 6358 was originally used with 1 inch to ¼ inch fittings to connect the test valve to the joining pipe-work. When the same valve and fittings were modelled using ANSYS CFX, the recirculation produced from the fittings made it difficult to simulate. For this reason the bore size was reduced to ¼ inch further away from the valve. Figure 14 shows a schematic diagram of the flow rig. A force-displacement meter was used to ensure valve A and valve B had the same stroke during testing. The stroke on each valve was measured at 0.62mm. Valve X is shown as a push button valve in the schematic as it was operated using a force displacement meter rather than a solenoid. Figure 16 shows the force displacement meter operating the valve. As with the CFD model, the inlet and outlet pressures were measured at 6 bar(g) ± 0.05 and 5 bar(g) ± 0.05 respectively. At these conditions the flow rate was measured using a positive displacement flow meter. The pressure and flow transmitters were connected to a data acquisition system. This ensured an acceptable level of experimental accuracy.

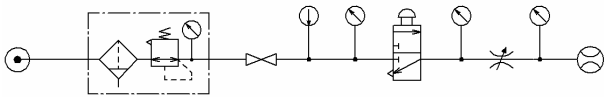

Fig. 14: *Schematic view of pneumatic flow rig*

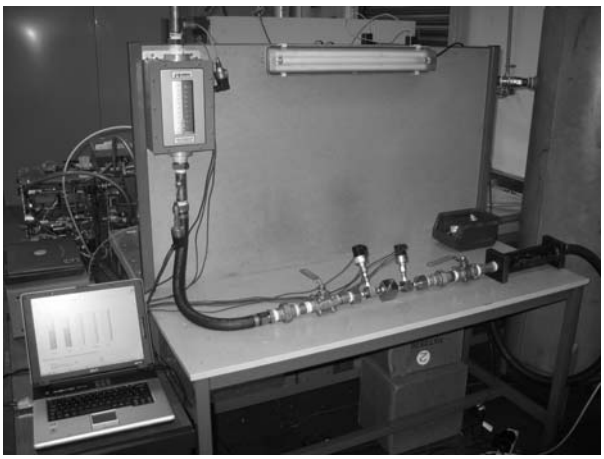

Fig. 15: *Pneumatic flow rig test on valve X*

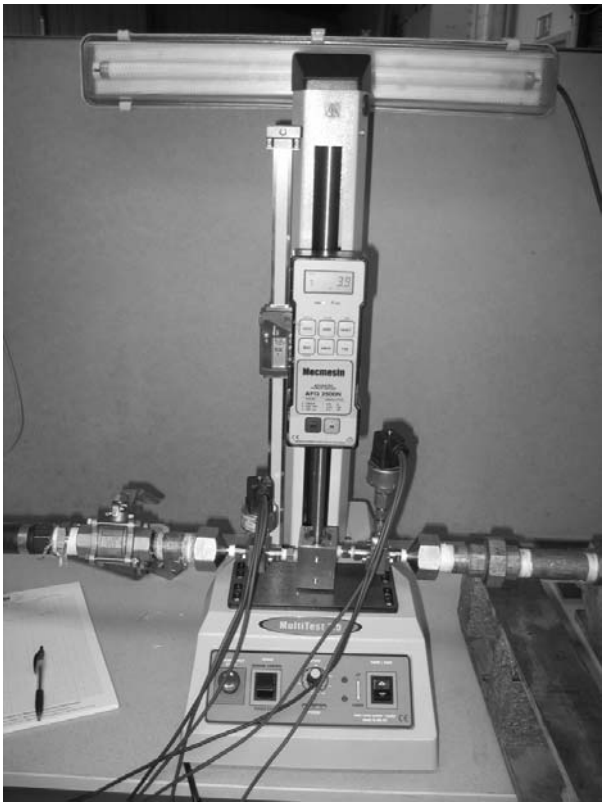

Fig. 16: *Force displacement meter used to ensure constant displacement*

3.2 Pneumatic Actuator Test

A 50 litre single acting spring return pneumatic actuator was used to compare the flow rates of valve A and valve B. It was decided to test the valves on a pneumatic actuator as this model of valve is commonly used in this type of application. The time taken to operate the actuator was measured using each valve. Figure 17 shows a schematic view of the pneumatic actuator test. Pressure readings were taken at the inlet to the actuator and the inlet to the valve. Figure 18 shows the pressure plots taken for each valve. When filling the actuator, the process can be split into three stages. During stage one, the volume remains fixed and the pressure increases until the force on the piston equals the force produced by the spring and the friction of the piston. During stage two, the piston begins to move and

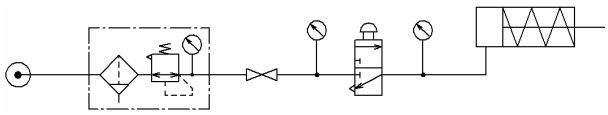

Fig. 17: *Schematic view of pneumatic actuator test*

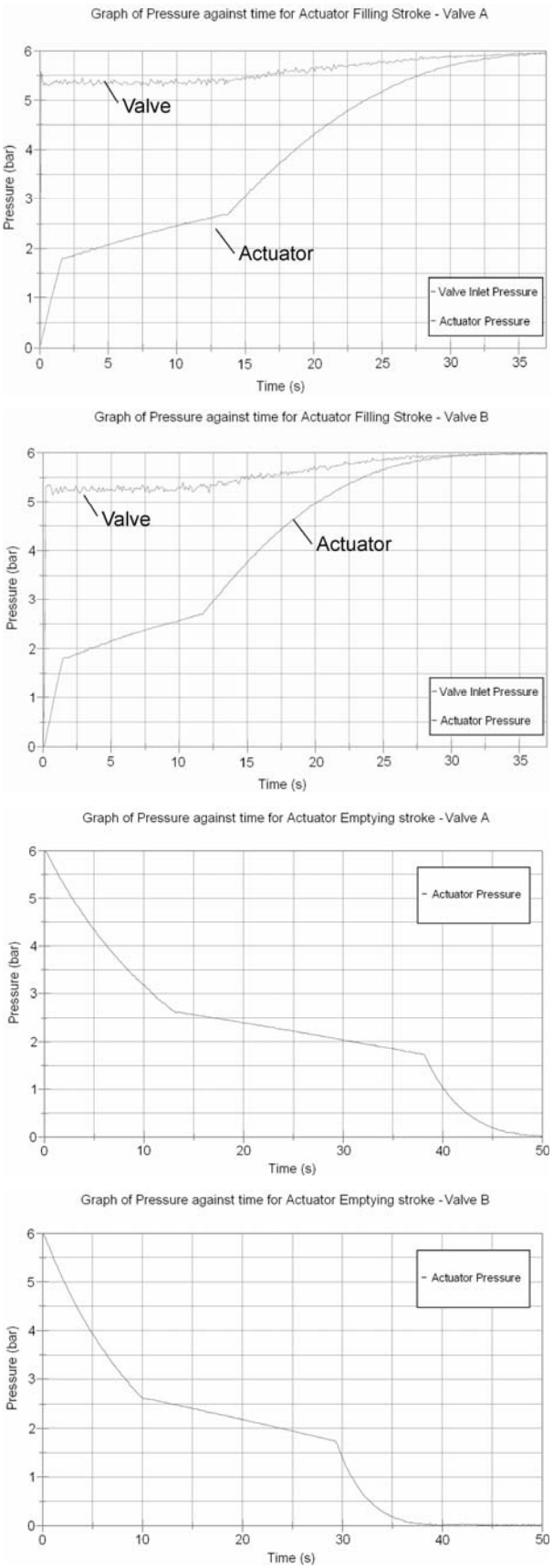

Fig. 18: *Pressure plots taken at inlet to pneumatic actuator*

the pressure continues to rise until the stroke of the piston is met. During stage three, the pressure inside the volume continues to rise until the set point of the filter regulator is met. The three stages can be seen in the graphs of the filling strokes. Similarly, when emptying the actuator, the process can be split into three stages. During stage one, the pressure decreases, until the pressure acting on the piston equals the spring force and friction force. During stage two the piston moves and the pressure decreases until the piston reaches the end of its stroke. During stage three, the pressure continues to fall to 0 bar(g). The three stages can be seen in the graphs of the emptying strokes. The times taken to fill and empty the actuator using valves A and B were read off the pressure plots.

3.3 Hydraulic Flow Test

Figure 19 shows a schematic view of the hydraulic flow rig. The flow rate and downstream pressure was measured using an analogue flow meter and digital pressure gauge. Measurements were taken at 2 and 4 bar(g) inlet..

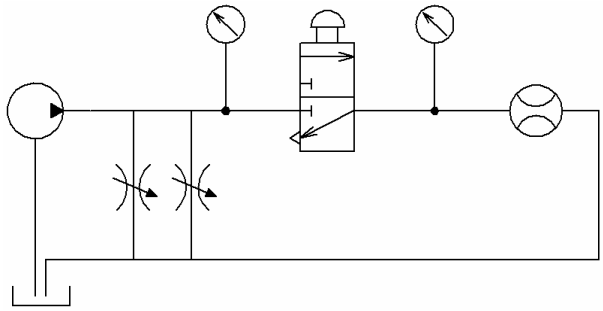

Fig. 19: *Schematic view of the hydraulic flow rig*

4 Overall Results

The overall results are presented in Table 3. We can see the percentage improvement in flow through the modified valve ranges from 11 % to 15 % for flow through ports 1-2 and from 16 % to 23 % for flow through ports 2-3. Also, both the pneumatic CFD and experimental pneumatic flow results were of similar magnitude in their improvement between the two valves.

Table 3a: Overall results - valve A, existing design - valve B, modified design. Flow through valve, ports 1-2

	Valve A	Valve B	% Improvement
Pneumatic CFD Results	0.01600 kg/s	0.01805 kg/s	12.8%
Hydraulic CFD Results	0.42014 kg/s	0.47263 kg/s	12.5%
Pneumatic Flow Results	0.01355 kg/s	0.01533 kg/s	13.1%
Hydraulic Flow Results (4 bar(g) inlet)	17.5 lpm	19.5 lpm	11.4%
Pneumatic Actuator Results	13.7 s	11.7 s	14.6%

Table 3b: Overall results - valve A, existing design - valve B, modified design. Flow through valve, ports 2-3

	Valve A	Valve B	% Improvement
Pneumatic CFD Results	0.01277 kg/s	0.01502 kg/s	17.6%
Hydraulic CFD Results	0.29960 kg/s	0.34598 kg/s	15.5%
Pneumatic Flow Results	0.01196 kg/s	0.01421 kg/s	18.8%
Hydraulic Flow Results	13.5 lpm	16.0 lpm	18.5%
Pneumatic Actuator Results	38.0 s	29.1 s	23.4%

5 Conclusion

The pneumatic CFD results gave 12.8 % improvement from ports 1-2 and 17.6 % improvement from ports 2-3.

The pneumatic flow test results gave 13.1 % improvement from ports 1-2 and 18.8% improvement from ports 2-3. This is a direct comparison with the CFD results, with 6 bar(g) inlet and 5 bar(g) outlet, and gives a strong correlation.

All results show a similar percentage increase in performance from valve A to valve B. They also show a higher percentage increase from 2-3 than from 1-2.

The results show that the changes to the geometry including rounding off edges and removing dead-space has a significant improvement on the amount of fluid flow rate going through the valve. This increase in mass flow rate through the valve is due to the reduction in head losses through the valve. CFD analysis can therefore be an effective tool in the design and optimisation of valves.

Optimization of the flow may have increased the force acting on the spool. The additional force is likely to be negligible, so no alterations should be required to the bottom spring or solenoid. It is also unlikely to have had a noticeable impact on the valves lifetime or opening time.

Acknowledgements

The first author is a Knowledge Transfer Partnership Associate on a scheme between Bifold Fluidpower Ltd and Manchester Metropolitan University and would like to thank all members of the partnership for their help and support in this project.

References

ANSYS CFX, Release 10.0: Installation and Overview, ANSYS

Bardina, J., **Ferziger, J. H.** and **Reynolds, W. C.** 1983. Improved turbulence models based on large eddy simulation of homogeneous, incompressible, turbulent flows. *Technical Report TF-19, Thermal sciences div., Dept. of Mech. Eng.*, Stanford Univ., Stanford, CA.

Bifold-Fluidpower, *Bifold-Fluidpower Corporate Catalogue* 2006. Bifold-Fluidpower.

Bredau, J. and **Helduser, S.** 1999. Numerical Flow Calculation in Pneumatics and Comparison with Measurement Results. *6th Scandinavian International Conference on Fluid Power*, SICFP'99, pp. 759-772.

Davis, J. A. and **Stewart, M.** 2002. Predicting Globe Controle Valve Performance – Part I: CFD Modeling. *ASME J. Fluids Eng.*, 124, pp. 772-777.

Davis, J. A. 2002. Predicting Globe Controle Valve Performance – Part II: Experimental Verification. *ASME J. Fluids Eng.*, 124, pp. 778-783.

Davis, J. A. and **Stewart, M.** 1998. Geometry Effects when using CFD Analysis as a Design Tool to Predict Control Valve Performance. *Developments in Theoretical and Applied Mechanics*, 19, pp. 38-45.

Huang, C. and **Kim, R. H.** 1996. Three Dimensional Analysis of Partially Open Butterfly Valve Flows. *ASME J. Fluids Eng.*, 118, pp. 562-568.

Ito, K., **Takahashi, K.** and **Inoue, K.** 1993. Flow in a Poppet Valve Computation of Pressure Distribution using Streamline Coordinate System. *JSME Inter-*

national Journal, 36, pp. 42-50.

Kerh, T., **Lee, J. J.** and **Wellford, L. C.** 1997. Transient Fluid – Structure Interaction in a Control Valve. *ASME J. Fluids Eng.*, 119, pp. 354-359.

Min, B., **Xin, F.** and **Ying, C.** 2001. Computational Fluid Dynamics Approach to Pressure Loss Analysis of Hydraulic Spool Valve. *Fifth International Conference on Fluid Power Transmission and Control*, ICFP 2001, Hangzhou, China.

Nadarajah, S., **Balabani, S.**, **Tindal, M. J.** and **Yianneskis, M.** 1998. The Turbulence Structure of the Annular Non-Swirling Flow Past an Axisymmetric Poppet Valve. *Proc. Inst. Mech. Eng.*, 212, pp. 455-472.

Nadarajah, S., **Balabani, S.**, **Tindal, M. J.** and **Yianneskis, M.** 1998. The Effect of Swirl on the Annular Flow Past an Axisymmetric Poppet Valve. *Proc. Inst. Mech. Eng.*, 212, pp. 473-484.

Roorda, O. 1998. Computer Simulation Helps Reduce Pressure Loss. *Water, Engineering and Management*, 40, pp. 22-24.

Salvador, G. P. and **Valverde, J. A.** 2004. Three-Dimensional control valve with Complex Geometry: CFD Modelling and Experimental Validation. *AIAA 2004 Fluid Dynamics Conference and Exhibit*, American Institute of Aeronautics and Astronautics.

Sullivan, J. A. 1975. *Fluid Power: Theory and Applications*. Reston Pub Co.

Yeaple, F. D. 1990. *Fluid Power Design Handbook*. Marcel Dekker Inc.

Nicholas Whitehead
is currently a Design Engineer at Bifold Fluidpower and is studying part time for an MPhil in Mechanical Engineering (Title: Assessment of Pneumatic and Hydraulic Valve Design through Fluid Flow Modelling). Arezki Slouti and Howard Taylor are his tutors. He graduated with a Masters degree in Mechanical Engineering from Manchester University in 2003.

Dr Arezki Slaouti
is currently a senior lecturer at the Department of Engineering and Technology from Manchester Metropolitan University. He obtained his PhD degree in Fluid Mechanics at the University of Manchester in 1980. He has research experience in Fluid Dynamics (Unsteady Separated Flows) and in Heat transfer involving numerical and experimental work stretching over 25 years. He has authored over thirty publications in refereed international journals and conference proceedings.